

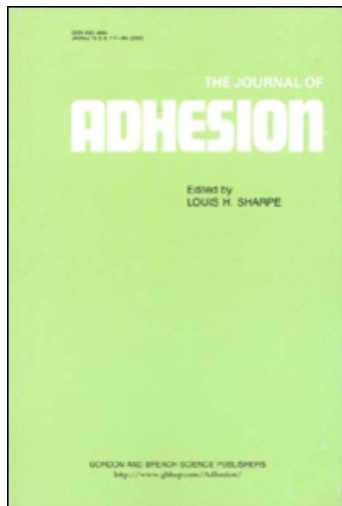
This article was downloaded by:

On: 22 January 2011

Access details: *Access Details: Free Access*

Publisher *Taylor & Francis*

Informa Ltd Registered in England and Wales Registered Number: 1072954 Registered office: Mortimer House, 37-41 Mortimer Street, London W1T 3JH, UK



## **The Journal of Adhesion**

Publication details, including instructions for authors and subscription information:

<http://www.informaworld.com/smpp/title~content=t713453635>

### **Multiaxial, temperature, and time-dependent (matt) failure model**

D. E. Richardson<sup>a</sup>; M. L. McLennan<sup>a</sup>; G. L. Anderson<sup>a</sup>; D. J. Macon<sup>a</sup>; A. Batista-Rodriguez<sup>a</sup>

<sup>a</sup> ATK Thiokol Propulsion Corporation, Brigham City, Utah

Online publication date: 08 September 2010

**To cite this Article** Richardson, D. E. , McLennan, M. L. , Anderson, G. L. , Macon, D. J. and Batista-Rodriguez, A.(2003) 'Multiaxial, temperature, and time-dependent (matt) failure model', *The Journal of Adhesion*, 79: 2, 157 – 174

**To link to this Article:** DOI: 10.1080/00218460309571

**URL:** <http://dx.doi.org/10.1080/00218460309571>

PLEASE SCROLL DOWN FOR ARTICLE

Full terms and conditions of use: <http://www.informaworld.com/terms-and-conditions-of-access.pdf>

This article may be used for research, teaching and private study purposes. Any substantial or systematic reproduction, re-distribution, re-selling, loan or sub-licensing, systematic supply or distribution in any form to anyone is expressly forbidden.

The publisher does not give any warranty express or implied or make any representation that the contents will be complete or accurate or up to date. The accuracy of any instructions, formulae and drug doses should be independently verified with primary sources. The publisher shall not be liable for any loss, actions, claims, proceedings, demand or costs or damages whatsoever or howsoever caused arising directly or indirectly in connection with or arising out of the use of this material.

## MULTIAXIAL, TEMPERATURE, AND TIME-DEPENDENT (MATT) FAILURE MODEL

**D. E. Richardson**  
**M. L. McLennan**  
**G. L. Anderson**  
**D. J. Macon**  
**A. Batista-Rodriguez**  
ATK Thiokol Propulsion Corporation,  
Brigham City, Utah

*The effects of multiaxial loading, temperature, and time on the failure characteristics of an adhesive are studied. This paper documents the use of extensive and varied test data in the development of a new multiaxial, temperature, and time-dependent (MATT) failure model. This new failure model employs a combination of the Tsai-Wu (or a modified Drucker Prager) failure criterion and a linear cumulative damage failure model. The model is developed using pure tensile and pure shear failure data. Verification of the accuracy of the model is evaluated using multiaxial and creep test data. Model development and verification testing was completed with a combination of tensile adhesion button and napkin ring test specimens. The model is shown to be very accurate for a wide range of load combinations, temperatures, and failure times.*

**Keywords:** Failure; Multiaxial; Temperature; Time; Adhesive

## INTRODUCTION

Extensive effort has been expended in a recent characterization of the effects of multiaxial loading, temperature, and time on the failure characteristics of an adhesive (a filled epoxy). In the past, the effects of each of these conditions were accounted for separately. This paper

Received 8 March 2002; in final form 2 July 2002.

A summary of this paper was presented at the 25th Annual Meeting of The Adhesion Society, Inc., held in Orlando, Florida, USA, 10–14 February, 2002.

Address correspondence to David E. Richardson, ATK Thiokol Propulsion Corporation, P.O. Box 707 M/S LE1, Brigham City, UT 84302-0707, USA. E-mail: david.richardson@thiokol.com

documents the use of the test data from this program in the development and evaluation of a combined multiaxial, temperature, and time-dependent (MATT) failure model. Verification of the failure model will also be presented.

## MATT FAILURE

The following MATT failure model is proposed and will be discussed in detail in this paper:

$$AP^2J_2 + BPI_1 = 1$$

In this equation,  $J_2$  is the second deviatoric stress invariant, and  $I_1$  is the first stress invariant. For an arbitrary stress state

$$J_2 = \frac{1}{3} \begin{bmatrix} \sigma_{11}^2 + \sigma_{22}^2 + \sigma_{33}^2 \\ -\sigma_{11}\sigma_{22} - \sigma_{11}\sigma_{33} - \sigma_{22}\sigma_{33} \\ + 3\sigma_{12}^2 + 3\sigma_{13}^2 + 3\sigma_{23}^2 \end{bmatrix}$$

$$I_1 = \sigma_{11} + \sigma_{22} + \sigma_{33}$$

A and B are shape parameters that define the ellipsoidal nature of the failure envelope. P is a scaling factor that scales the failure envelope to a proper level for a given temperature and failure time. Determination of each of these parameters will be discussed in detail in the following sections.

As can be seen from the equations given above, for a constant P value this failure model is equivalent to the Tsai-Wu failure model [1] that is traditionally used in the evaluation of composite materials. With a constant P, the model is also equivalent to a modified Drucker Prager failure model [2].

The use of the P scaling factor makes the criterion unique. The P scaling factor takes into account the temperature and time dependence of the material being modeled. As will be discussed in the next sections, this factor will be modeled using a linear cumulative damage technique [3].

## ADHESIVE SYSTEM

The adhesive used in this study is a commercially available aliphatic amine-cured epoxy. Fiber and powder fillers are used in the formulation to provide thixotropic behavior and increase the fracture energy of the adhesive. The adhesive was vacuum-mixed and cured with standard procedures.

Surface preparation of the metal substrates used for testing entailed an aqueous detergent wash followed by grit blasting using a commercially available aluminum silicate. A silane primer was applied to the grit-blasted bond surfaces in order to improve adhesion.

## TENSILE ADHESION

The first step in understanding and developing the failure model is to discuss tensile adhesion failure data. The results of this testing have been documented earlier in more detail [4, 5] and are only included here for reference.

The tensile adhesion testing was completed using a tensile adhesion button specimen (Figure 1).

Tensile adhesion tests were conducted at temperatures ranging from  $-29^{\circ}\text{C}$  to  $46^{\circ}\text{C}$  ( $-20^{\circ}\text{F}$  to  $115^{\circ}\text{F}$ ) and at load rates that had failure times ranging from minutes to days. No time dependence in failure for this adhesive was observed for temperatures below  $4^{\circ}\text{C}$  ( $40^{\circ}\text{F}$ ), well below the glass transition temperature. The constant load rate test data were used to develop a linear cumulative damage failure model [3–5] of the following form:

$$N_{\sigma} = \left[ \int_0^{t_f} \sigma_i^{\beta} dt \right]^{1/\beta}$$

where  $N_{\sigma}$  and  $\beta$  are experimentally determined failure parameters,  $\sigma_i$  is an applied stress as a function of time with a corresponding failure time  $t_f$ .  $N_{\sigma}$  is a characteristic measure of the capability of the material and represents the accumulation of damage in the material, and  $\beta$  defines the level of damage being accumulated for a given stress level in the load history. For a constant rate load history,  $\beta$  is the slope of the strength versus time curve in log-log space.

In the case of constant tensile-stress rate loading (used for this testing) with a rate of  $\dot{\sigma}$ , the stress at any time is given by

$$\sigma_i(t) = \dot{\sigma}t$$

Using the above equations, the failure time ( $t_f$ ) and failure stress ( $\sigma_f$ ) can be shown to be

$$t_f = (1 + \beta) \left[ \frac{N_{\sigma}}{\sigma_f} \right]^{\beta}$$

$$\sigma_f = N_{\sigma} \left[ \frac{t_f}{1 + \beta} \right]^{\frac{-1}{\beta}}$$

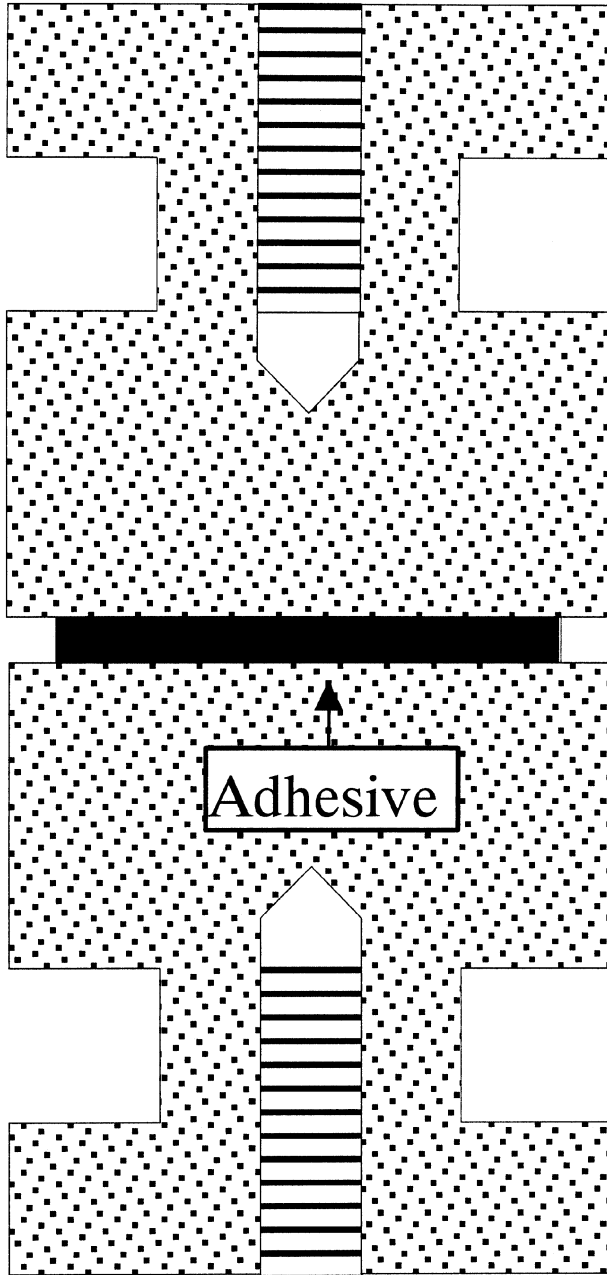


**FIGURE 1** Tensile adhesion button.

As can be seen in the equations, the log of the failure stress is a linear function of the log of the failure time. Failure data can be plotted in log(stress)-log(time) space to the following form:

$$\log(\sigma_f) = m \log(t_f) + b$$

where  $m$  is the slope and  $b$  is the intercept.  $N_\sigma$  and  $\beta$  can be evaluated from the relation given above using the following relationships:

$$\beta = \frac{-1}{m} \quad N_\sigma = 10^{\frac{b - \log(1+\beta)}{\beta}}$$

Test data ranging from 21°C to 46°C (70°F to 115°F) are shown in Figure 2. The linear nature of the failure data described above can be seen in the figure. This linear relationship holds for each temperature. It should be noted that these test temperatures are below the glass transition temperature. It is doubtful that this linear trend would hold through the glass transition, especially for under-cured adhesives.

Using the slopes and intercepts obtained from the curve fits seen in Figure 2, the  $N_\sigma$  and  $\beta$  values for each temperature are obtained using the equations above. Both  $N_\sigma$  and  $\beta$  vary linearly with temperature as shown in Figures 3 and 4.

If the linear relationships derived from these figures are input into the cumulative damage failure model, a single temperature and

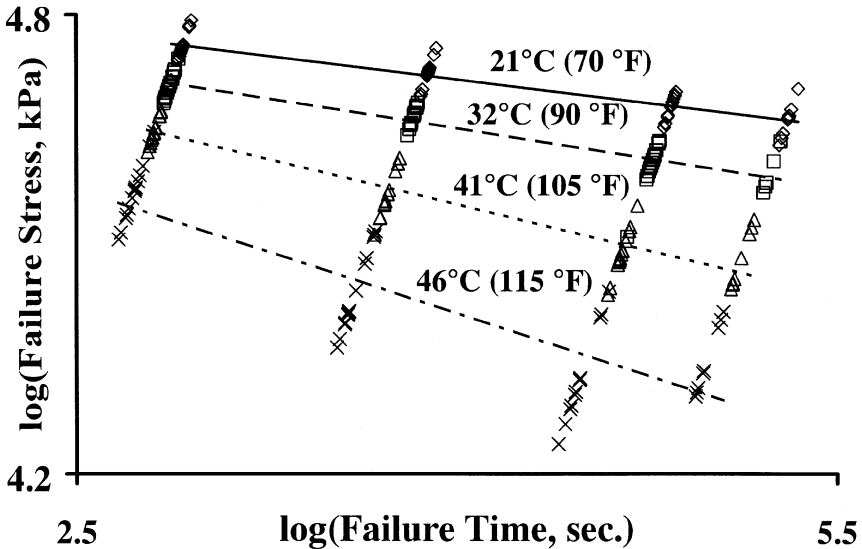


FIGURE 2 Tensile button failure data.

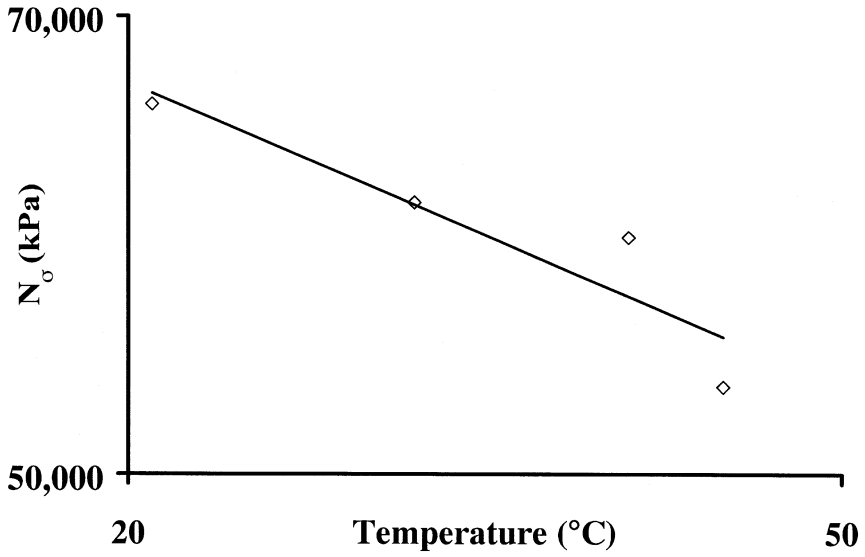


FIGURE 3  $N_{\sigma}$  versus temperature.

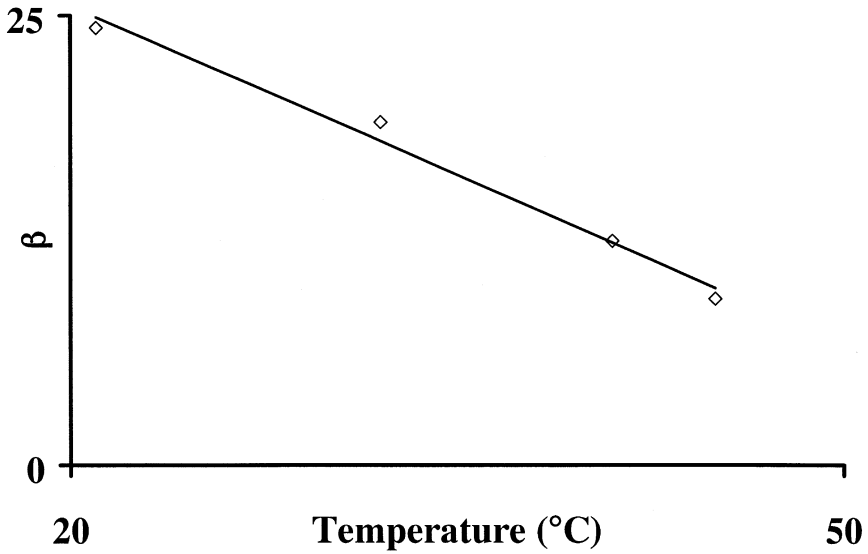


FIGURE 4  $\beta$  versus temperature.

time-dependent failure model is developed for the analyzed temperatures and times.

## VERIFICATION OF TEMPERATURE AND TIME CHARACTERIZATION

Prior to proceeding with the development of the MATT failure criterion, it is important to review the testing that was completed to verify the time and temperature-dependent failure model [5]. Creep resistance testing using tensile adhesion buttons was performed to provide this verification.

Using the linear cumulative damage relation described above, failure times and stresses can be predicted for constant stress conditions:

$$\sigma_i(t) = \text{constant} = \sigma_k$$

$$t_f = \left( \frac{N_\sigma}{\sigma_k} \right)^\beta \quad \sigma_f = N_\sigma t_f^{-\frac{1}{\beta}}$$

Predictions of creep failure conditions can be seen in Figures 5–8 (for comparison purposes, all plots have equivalent axis definitions). Failure times range from less than 1 h to approximately 5 months. The

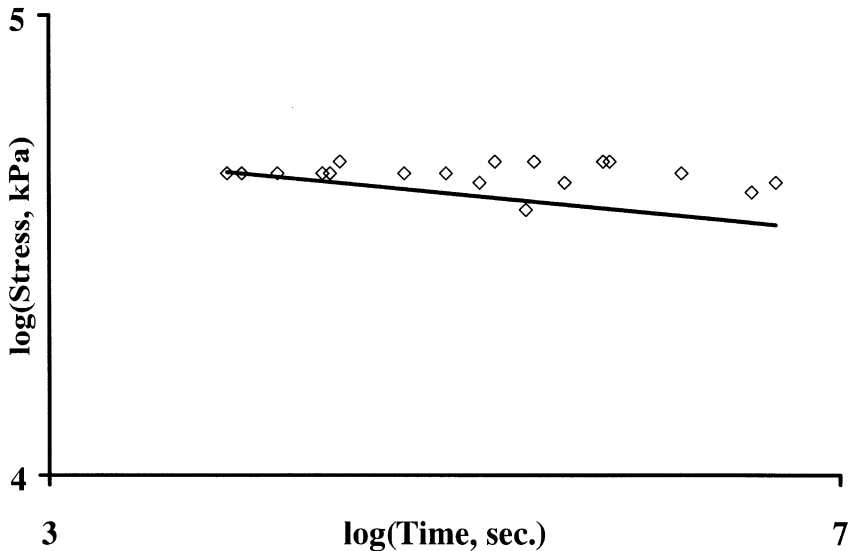


FIGURE 5 Creep data and predictions for 21°C (70°F).



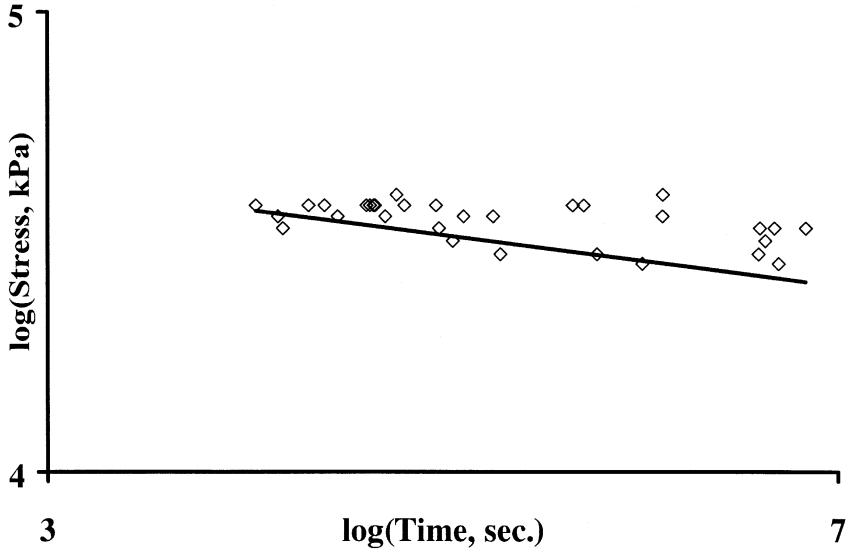


FIGURE 6 Creep data and predictions for 32°C (90°F).

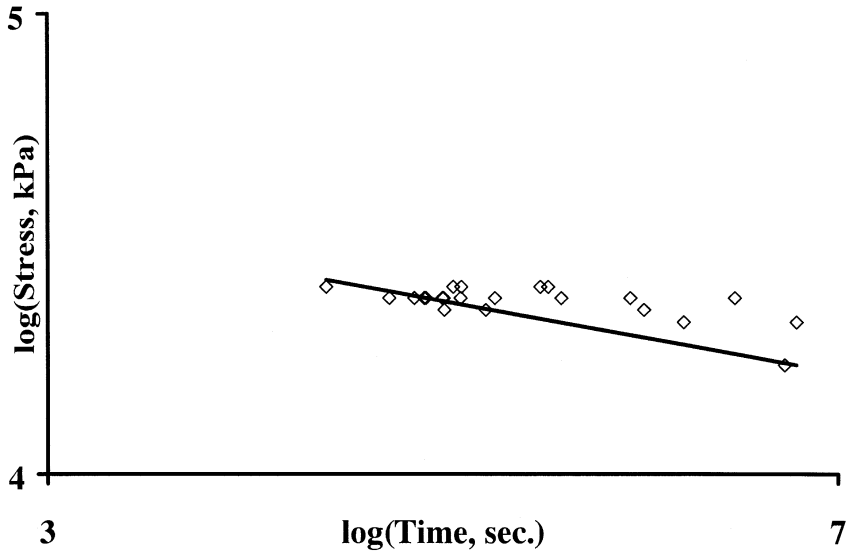
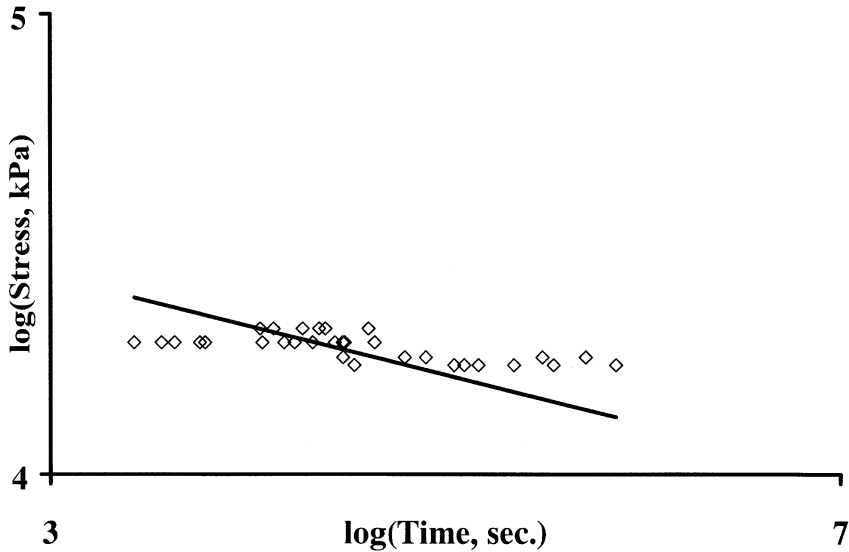


FIGURE 7 Creep data and predictions for 41°C (105°F).



**FIGURE 8** Creep data and predictions for 46°C (115°F).

test data indicate that the characterization of the time and temperature dependence was successful (and conservative) over this wide range of times and temperatures.

### **SHEAR ADHESION**

The time and temperature dependence of shear failure was also characterized using napkin ring shear adhesion specimens (see Figure 9) [6–8]. Similar to the tensile adhesion testing, the shear adhesion tests were conducted at temperatures ranging from  $-29^{\circ}\text{C}$  to  $46^{\circ}\text{C}$  ( $-20^{\circ}\text{F}$  to  $115^{\circ}\text{F}$ ) and at load rates that had failure times ranging from minutes to days.

To evaluate the multiaxial nature of adhesive failure, predictions were made of average tensile adhesion button failure loads (using the cumulative damage failure model) for the same temperature and failure times as the constant shear load rate test. The ratios of these failure loads can be seen in Table 1. The load rates in the table differ by an order of magnitude (load rate #1 is two orders of magnitude faster than load rate #3).

Note that the ratio between the shear data and the tensile data is nearly constant at (0.80) for several temperatures and load rates. This leads to the conclusion that shear failure for the adhesive can be predicted for any temperature and failure time (within the range

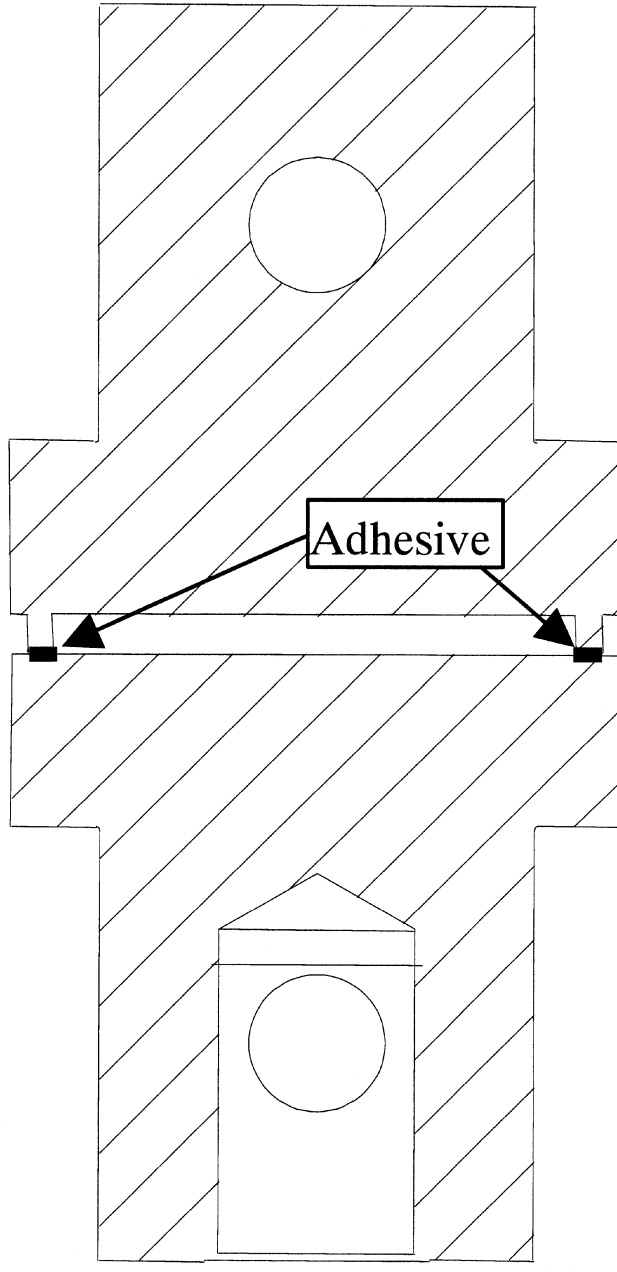


**FIGURE 9** Napkin ring test specimen.

**TABLE 1** Ratio of Shear/Tensile

Temperature	Load rate	Ratio
21°C (70°F)	#1	0.81
21°C (70°F)	#2	0.79
21°C (70°F)	#3	0.77
32°C (90°F)	#1	0.81
32°C (90°F)	#2	0.82
32°C (90°F)	#3	0.79
41°C (105°F)	#1	0.79
41°C (105°F)	#2	0.83
41°C (105°F)	#3	0.82
46°C (115°F)	#1	0.78
46°C (115°F)	#2	0.83
46°C (115°F)	#3	0.86

tested) if the tensile strength is known for the same temperature and failure time. This is accomplished by using the cumulative damage equations presented above where:

$$\tau_f(T, t_f) = 0.8\sigma_f(T, t_f)$$

The accuracy of this relationship can also be seen in Figure 10. Similar accuracy was noted for tests conducted at 32°C and 41°C (90°F and 105°F).

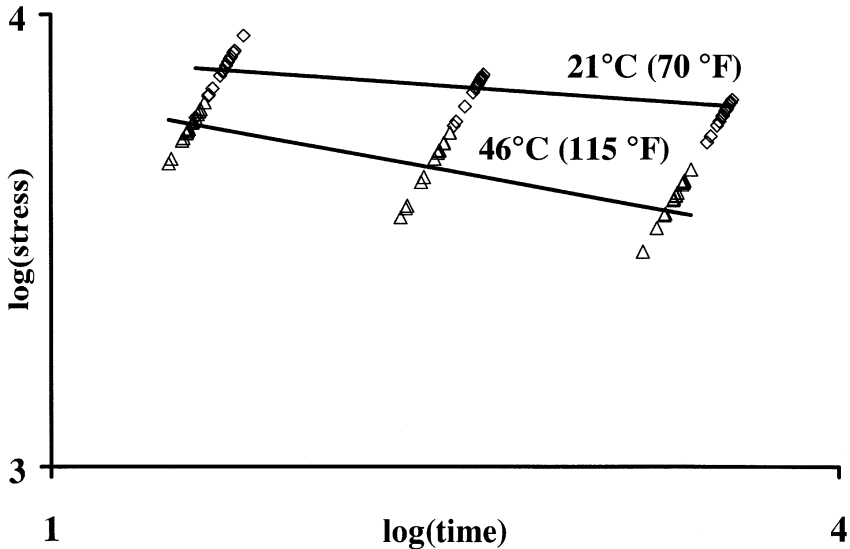


**FIGURE 10** Shear data and prediction.

## MULTIAXIAL

Two important points can be made from the tensile and shear data. First, it can be seen that the ratio between the tensile adhesion and the shear adhesion failure is constant and independent of time and temperature. This leads to the conclusion that the shape of the failure surface (not the size) is independent of temperature and failure time. Hence the A and B shape factors in the MATT equation can be used to define the shape of the failure surface.

The second major point is that the tensile and shear adhesion temperature and time dependence appear to be equivalent. This leads to the conclusion that the failure ellipse can be scaled to appropriate levels for a given temperature and failure time. Thus, the scaling factor, P, can be used to define the size of the failure ellipse.

It is not clear if these conclusions and the described relationships will hold valid near or above the glass transition.

As discussed earlier, the failure surface generated by this failure criterion is elliptical in shape. The coefficients can be determined if two data points are provided for a given failure time and temperature. Therefore, the basic shape of the failure surface for this adhesive is defined by the fact that the shear adhesion strength is 80% of the tensile adhesion strength.

The napkin ring specimen induced a nearly pure shear loading condition, but the tensile adhesion button has a multiaxial loading condition. By finite element analyses it can be shown that the tensile adhesion button will have the following peak stresses during loading:

$$\begin{aligned}\sigma_{11} &= 1.04(\sigma_f) \\ \sigma_{22} = \sigma_{33} &= 0.61(\sigma_{11}) \\ \tau_{12} = \tau_{13} = \tau_{23} &= 0.0\end{aligned}$$

If it is assumed that  $\tau_f = 1.0$  and  $\sigma_f = 1.25$  ( $\tau_f = 0.8\sigma_f$ ), then it can be shown that

$$\begin{aligned}A &= 1.0 \\ B &= 0.31754\end{aligned}$$

The magnitude of the scale factor, P, can be found for any application if the temperature and time-dependent failure is characterized for a specific stress state. For this study, the temperature and time dependence of tensile adhesion failure is known and utilized.

Theoretically, any other loading conditions may be used (e.g., uniaxial or shear). The P in the MATT failure criterion is the factor which forces the failure surface to pass through the known failure value

(tensile adhesion for this study) for a given temperature and failure time.

For this study in which tensile adhesion button data were used, it was important to account for the triaxial state of stress in the bondline for all temperature and time conditions. This can be completed through closed-form solutions of the stress state or through finite element analyses.

If the above noted A and B values are used in conjunction with the tensile adhesion failure values for cold temperatures,  $-29^{\circ}\text{C}$  to  $4^{\circ}\text{C}$  ( $-20^{\circ}\text{F}$  to  $40^{\circ}\text{F}$ ), or the cumulative damage model for warm temperatures,  $21^{\circ}\text{C}$  to  $46^{\circ}\text{C}$  ( $70^{\circ}\text{F}$  to  $115^{\circ}\text{F}$ ), failure can be predicted for any load combination, temperature, or failure time. If this MATT failure criterion is used to predict the tensile adhesion and shear adhesion failure data between  $21^{\circ}\text{C}$  and  $46^{\circ}\text{C}$  ( $70^{\circ}\text{F}$  and  $115^{\circ}\text{F}$ ) described in this report, the coefficient of variation is 9.3%. This low coefficient of variation indicates that the failure model provides a very good fit of the failure data for both tensile and shear loadings, under different temperatures, and for a wide range of failure times.

## VERIFICATION OF MULTIAXIAL

The temperature and failure time dependency was verified with the tensile, shear, and creep data discussed earlier. The multiaxial nature of the failure theory is verified using separate multiaxial test data generated with the napkin ring specimen [6–8]. The test specimens were loaded with both normal and shear stresses. The raw test data and the MATT prediction can be seen in Figures 11–15. As can be seen, the predictions accurately match the test data.

## EXAMPLE

To show the utility and simplicity of the model, two examples are presented. Assume that a factor of safety needs to be calculated for a specific stress state,  $\sigma_i^*$  (with corresponding  $J_2^*$  and  $I_1^*$ ), that is held at a constant temperature,  $T^*$ , and held at a constant load for an evaluation time of  $t^*$ .

For this example, it is assumed that the A and B shape factors have been determined and that the time and temperature dependence of a uniaxial test specimen has been characterized. For simplicity, uniaxial failure is used in this example, not tensile adhesion failure (the condition that has been characterized in this study). Once again, the loading condition used to characterize the temperature and time dependence can be with any combination of stresses.

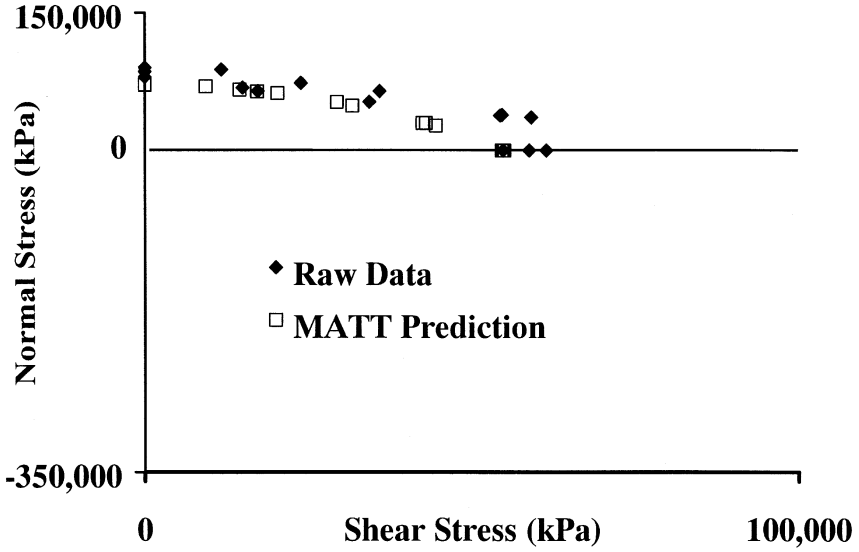


FIGURE 11 Predicted multiaxial,  $-7^{\circ}\text{C}$  ( $20^{\circ}\text{F}$ ).

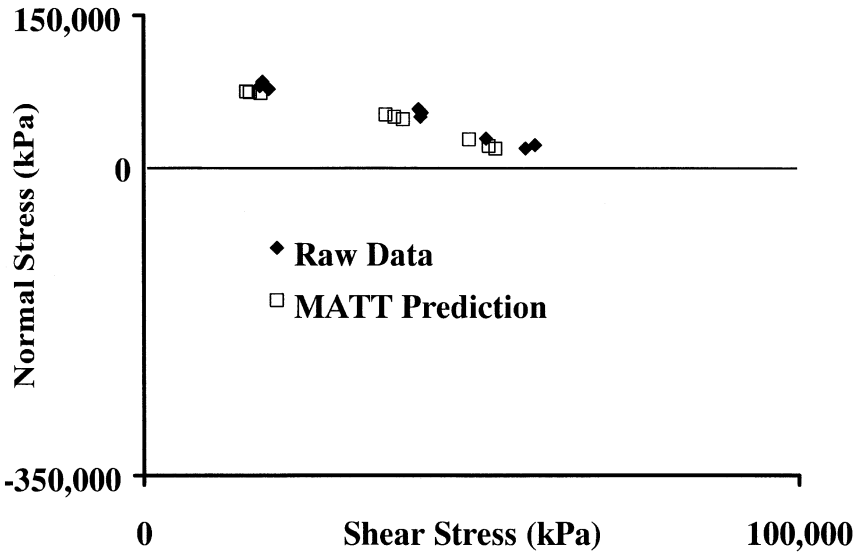


FIGURE 12 Predicted multiaxial,  $4^{\circ}\text{C}$  ( $40^{\circ}\text{F}$ ).

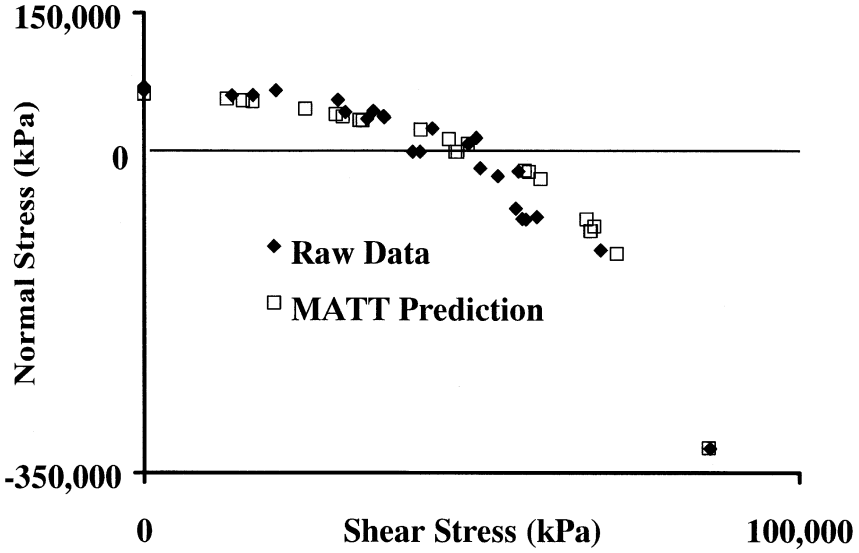


FIGURE 13 Predicted multiaxial, 21°C (70°F).

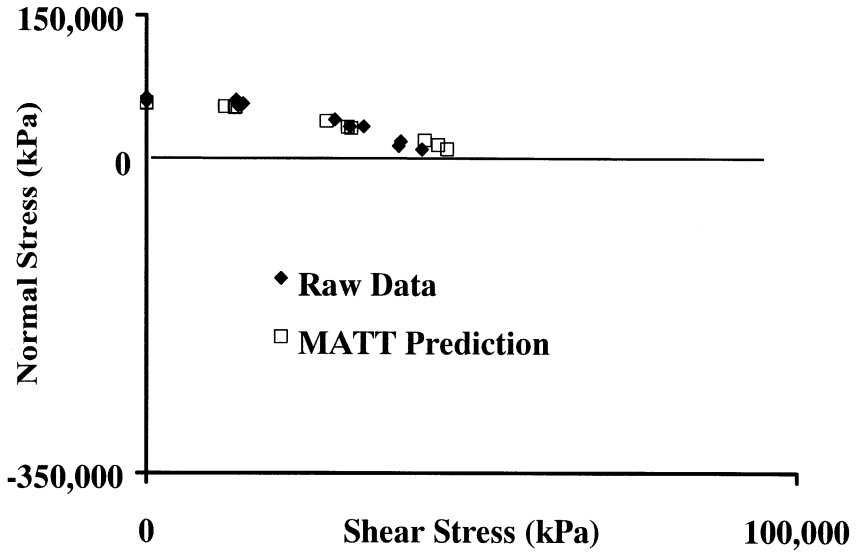


FIGURE 14 Predicted multiaxial, 32°C (90°F).



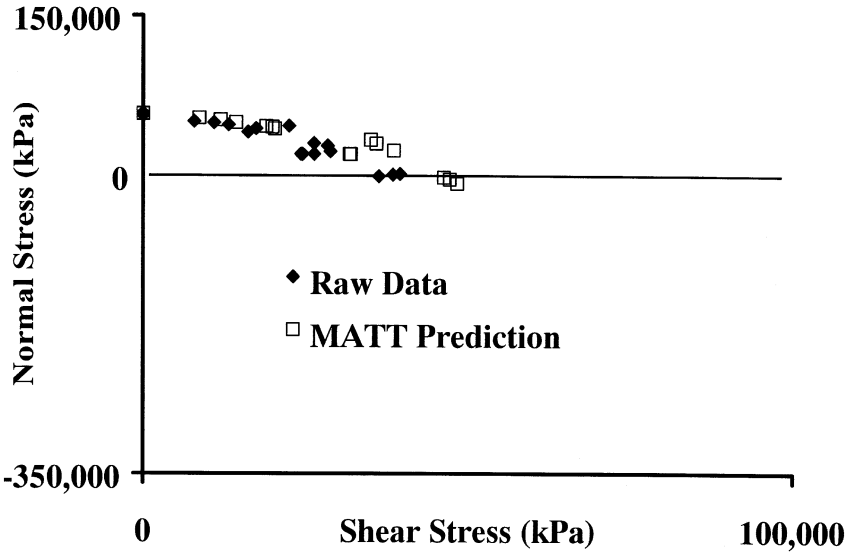


FIGURE 15 Predicted multiaxial, 46°C (115°F).

Before the factor of safety can be calculated, the P scaling factor must be determined. Using the linear cumulative damage failure model for constant load conditions, the failure stress of the material in uniaxial loading is found using the equations described above to be as follows:

$$\sigma_f^{\text{uniaxial}} = N_\sigma t^{*\frac{1}{\beta}}$$

where the appropriate temperature-dependent  $N_\sigma$  and  $\beta$  are used. The P factor is determined to be the factor that will cause the MATT failure surface to pass through this point. For a uniaxial load,

$$J_2^* = (\sigma_f^{\text{uniaxial}})^2$$

$$I_1^* = \sigma_f^{\text{uniaxial}}$$

P can be shown to be

$$P = \frac{-B\sigma_f^{\text{uniaxial}} + \left[ (B\sigma_f^{\text{uniaxial}})^2 + 4A(\sigma_f^{\text{uniaxial}})^2 \right]^{1/2}}{2A(\sigma_f^{\text{uniaxial}})^2}$$

Now that the MATT failure surface is defined (A, B, and P are known), the factor of safety (FS) can be calculated by solving the following quadratic equation:

$$AP^2 J_2^*(FS)^2 + BPI_1^*(FS) = 1$$

A similar approach can be used to predict the time to failure for a given stress state,  $\sigma_i^*$  (with corresponding  $J_2^*$  and  $I_1^*$ ) and constant temperature,  $T^*$ . In this case, the P scale factor that causes the MATT failure curve to pass through the specified stress state is determined:

$$P = \frac{-BI_1^* + [(BI_1^*)^2 + 4A(J_2^*)^2]^{1/2}}{2A(J_2^*)^2}$$

Using the given A, B, shape factors, and the P scaling factor, the uniaxial failure stress that passes through the same MATT failure surface can be found using:

$$\sigma_f^{\text{uniaxial}} = \frac{-BP + [(BP)^2 + 4AP^2]^{1/2}}{2AP^2}$$

The failure time is then calculated using the linear cumulative damage model:

$$t_f = \left( \frac{N_\sigma}{\sigma_f^{\text{uniaxial}}} \right)^\beta$$

given that the appropriate temperature-dependent  $N_\sigma$  and  $\beta$  are used.

## CONCLUSIONS

A multiaxial, temperature, and time-dependent failure criterion has been proposed and evaluated for an epoxy adhesive. The failure criterion has been shown to be applicable for temperatures ranging from  $-29^\circ\text{C}$  to  $46^\circ\text{C}$  ( $-20^\circ\text{F}$  to  $115^\circ\text{F}$ ), and has been shown to predict multiaxial failure accurately for constant load rate and constant load test specimens with failure times ranging from minutes to months. The failure criterion is general and can likely be extended to other material systems.

## REFERENCES

- [1] Tsai, S. W. and Wu, E. M., *J. Compos. Mater.*, **5**, 58–63 (1971).
- [2] Drucker, D. C. and Prager, W., *Q. Appl. Math.*, **10**, 157–165 (1952).
- [3] Laheru, K. L., *J. Propuls. Power*, **8**, 756–759 (1992).
- [4] Batista-Rodriguez, A. and Richardson, D. E., 2001 JANNAF Rocket Nozzle Technology Subcommittee Meeting, CPIA Pub. 707, 171–179, Cocoa Beach, Florida, (2001).

- [5] Richardson, D. E., Batista-Rodriguez, A., Macon, D. J. and Totman, P. D., 37th AIAA/ASME/SAE/ASEE Joint Propulsion Conference & Exhibit, AIAA Paper 2001-3720, 1–8, Salt Lake City, Utah, (2001).
- [6] Anderson, G. L., Crook, R. A., Richardson, D. E. and Boothe, R. E., Summer Meeting of the American Society of Mechanical Engineering, Oral Presentation, 185–193 Blacksburg, Virginia, (1999).
- [7] McCarvill, W. T. and Bell, J. P., *J. Adhesion*, **6**, 185 (1974).
- [8] Bryant, R. W. and Dukes, W. A., *Br. J. Appl. Phys.*, **16**, 101–108 (1965).